THE JOURNAL OF BIOLOGICAL CHEMISTRY VOL. 287, NO. 47, pp. 39554–39563, November 16, 2012

ADAMTS-12 Metalloprotease Is Necessary for Normal Inflammatory Response*[S]

Received for publication, August 7, 2012, and in revised form, September 25, 2012 Published, JBC Papers in Press, September 27, 2012, DOI 10.1074/jbc.M112.408625

Angela Moncada-Pazos[‡1,2], Alvaro J. Obaya[§1], María Llamazares[‡], Ritva Heljasvaara[‡¶3], María F. Suárez[‡], Enrique Colado[‖], Agnès Noël[**], Santiago Cal[‡], and Carlos López-Otín[‡]

From the [‡]Departamento de Bioquímica y Biología Molecular and [§]Biología Funcional, Instituto Universitario de Oncología (IUOPA), Universidad de Oviedo, 33006 Oviedo, Spain, the [¶]Oulu Center for Cell-Matrix Research, Biocenter Oulu and Department of Medical Biochemistry and Molecular Biology, University of Oulu, 90570 Oulu, Finland, the [‖]Servicio de Hematología, Hospital Universitario Central de Asturias, 33006 Oviedo, Spain, and the [**]Groupe Interdisciplinaire de Génoprotéomique Appliquée-Cancer (GIGA-Cancer)-Transgenesis, University of Liège, Tour de Pathologie, B-4000 Liège, Belgium

Background: ADAMTS-12 is a metalloprotease of unknown biological function. Mice deficient in *Adamts12* show no obvious phenotype.
Results: *Adamts12*-deficient mice exhibit increased inflammatory response and reduced neutrophil apoptosis.
Conclusion: This protease is necessary for resolution of inflammation allowing normal neutrophil apoptosis.
Significance: ADAMTS-12 has a role in inflammation, contributing to better understanding of the etiology of inflammatory diseases.

ADAMTSs (a disintegrin and metalloprotease with thrombospondin domains) are a family of enzymes with both proteolytic and protein interaction functions, which have been implicated in distinct pathologies. In this work, we have investigated the putative role of ADAMTS-12 in inflammation by using a mouse model deficient in this metalloprotease. Control and mutant mice were subjected to different experimental conditions to induce colitis, endotoxic sepsis, and pancreatitis. We have observed that *Adamts12*-deficient mice exhibit more severe inflammation and a delayed recovery from these challenges compared with their wild-type littermates. These changes are accompanied by an increase in inflammatory markers including several cytokines, as assessed by microarray expression analysis and proteomic-based approaches. Interestingly, the clinical symptoms observed in *Adamts12*-deficient mice are also concomitant with an elevation in the number of neutrophils in affected tissues. Finally, isolation and *in vitro* culture of human neutrophils demonstrate that the presence of ADAMTS-12 induces neutrophil apoptosis. On the basis of these results, we propose that ADAMTS-12 is implicated in the inflammatory response by modulating normal neutrophil apoptosis.

Metalloproteases regulate many biological processes in all living organisms through their ability to specifically cleave peptide bonds in a variety of substrates (1). Among them, the ADAMTSs[4] (a disintegrin and metalloprotease with thrombospondin domains) are a family of 19 secreted metalloproteases showing structural similarities to MMPs (matrix metalloproteinases) and ADAMs (a disintegrin and metalloprotease) such as the presence of a zinc-chelating motif essential for the enzymatic activity. However, the occurrence of different thrombospondin domains within their architecture represents a distinctive structural hallmark of ADAMTSs (2, 3). These thrombospondin domains, together with other ancillary motifs, constitute a region that likely acts by modulating substrate binding, determining cell location or sequestering factors in the extracellular matrix. Some ADAMTSs, such as ADAMTS-4 and ADAMTS-5, have been related to inflammatory-related processes including arthritic diseases (4). Therefore, it is tempting to speculate that the altered function of any of these ADAMTSs putatively involved in inflammation could contribute to the development of a variety of human diseases. In this regard, it is well established that abnormal and persistent immune responses are responsible for pathologies such as inflammatory bowel diseases, rheumatoid arthritis, atherosclerosis, or allergies. All of these conditions have increased their prevalence during the past decades and now constitute a major concern for public health with limited therapeutic opportunities (5). There is growing evidence that these pathologies are caused by a complex interaction between multiple susceptibility loci and environmental factors. Accordingly, identification of genes involved in inflammatory diseases and further characterization of their mechanisms of action represent suitable strategies for future clinical improvement of these conditions.

ADAMTS-12 was first identified and cloned in our laboratory in 2001 (6), although little is known concerning its normal

* This work was supported by grants from Ministerio de Economía y Competitividad-Spain, Fundación M. Botín and European Union (FP7-Micro-EnviMet). The Instituto Universitario de Oncología is supported by Obra Social Cajastur and Acción Transversal del Cáncer-RTICC.
[S] This article contains supplemental Figs. 1 and 2.
[1] Both authors contributed equally to this work.
[2] To whom correspondence should be addressed. Tel.: 34-985102747; E-mail: amoncada@degradome.uniovi.es.
[3] Supported by grants from Finnish Cultural Foundation and Maud Kuistila Memorial Foundation.

[4] The abbreviations used are: ADAMTS, a disintegrin and metalloprotease with thrombospondin domains; ADAM, a disintegrin and metalloprotease; DSS, dextran sulfate sodium; DiGE, differential gel electrophoresis; EBNA, Epstein Barr virus nuclear antigen; IEF, isoelectrofocusing; MMP, matrix metalloproteinase; MPO, myeloperoxidase; PI, propidium iodide.

biological functions. In contrast, there is growing information about the putative pathological relevance of this enzyme. ADAMTS-12 has been associated with osteoarthritis due to its ability to degrade the cartilage components aggrecan and cartilage oligomeric matrix protein (7, 8) and has been genetically related to rheumatoid arthritis (9). Moreover, ADAMTS-12 has been genetically linked to schizophrenia and asthma (10, 11). In neoplastic diseases, ADAMTS-12 has been described to act as an anti-tumor protease. In this regard, we have previously reported that this metalloprotease inhibits pro-tumor activities of Madin-Darby canine kidney and bovine aortic endothelial cells as well as *in vivo* growth of A549 tumor cells in SCID mice (7). Furthermore, *ADAMTS12* is hypermethylated in tumors from different origins, and, at least in colorectal cancer, the epigenetic silencing occurring in tumor cells is compensated by its overexpression in myofibroblasts of the surrounding stroma (12, 13). To try to elucidate the biological roles of this enzyme, we have recently established a mouse strain lacking *Adamts12*, which shows no obvious phenotype but exhibits significant differences in cancer susceptibility compared with control mice (14). Thus, *Adamts12*-deficient mice are more susceptible to cancer development, displaying increased angiogenesis and tumor invasion.

In the present work, we have studied the putative role of ADAMTS-12 in inflammation. For that purpose, we have examined the mouse model lacking *Adamts12* under distinct inflammatory conditions including ulcerative colitis, sepsis, and pancreatitis, with the finding that the absence of this protease causes increased inflammation. Moreover, we have analyzed the inflammatory response of *Adamts12*-deficient tissues at the molecular level and observed that several inflammatory markers are also increased at both RNA and protein levels and correlate with the observed clinical features. Finally, we have found that *Adamts12*-null mice undergo an excessive accumulation of neutrophils due to their reduced apoptosis. On the basis of these results, we propose that ADAMTS-12 exerts a protective role in inflammatory pathologies, avoiding a detrimental concentration of neutrophils by inducing their appropriate apoptosis.

EXPERIMENTAL PROCEDURES

Animals—*Adamts12*$^{-/-}$ mice were generated and genotyped as described previously (14). Briefly, exons 6 and 7 were replaced by a neomycin-phosphoglycerate kinase cassette through homologous recombination, causing introduction of a frameshift. The embryonic stem cells generated were then injected into C57BL/6J blastocysts. Animals were housed under specific pathogen-free conditions; all experiments were carried out at an age of 8–10 weeks and following the guidelines of the Committee on Animal Experimentation of the Universidad de Oviedo, Oviedo, Spain.

Induction of Colitis—27 *Adamts12*$^{+/+}$ and 33 *Adamts12*$^{-/-}$ mice were treated with 2% dextran sulfate sodium salt (DSS; MP Biomedicals) in drinking water for 7 days, followed by 1 day of water. Body weight and colitis clinical symptoms were monitored daily. At days 0, 3, 6, and 8, mice were sacrificed, and their colons were removed, measured, and washed to obtain colonic lavages. Afterward, colons were processed for histological analysis or frozen for protein extraction. An additional group of 14 *Adamts12*$^{+/+}$ and 15 *Adamts12*$^{-/-}$ mice was subjected to the same protocol to determine mortality rates and to estimate the degree of affectation at day 16, when initial weight was recovered.

LPS-induced Sepsis Model—36 *Adamts12*$^{-/-}$ and 38 *Adamts12*$^{+/+}$ mice were injected intraperitoneally with 8.5 mg/kg body weight of lipopolysaccharide (LPS; Sigma) in saline solution. Body weight was monitored daily. At days 2, 3, and 8, a minimum of 8 mice were anesthetized, and blood samples were taken by intracardiac puncture. Animals were then sacrificed and liver and spleen removed. Cell population abundances in blood were determined in the hematology analyzer Abacus Junior Vet (Diatron) and by flow cytometry using a combination of specific antibodies against murine CD45 (BD Biosciences 550994), CD45R (552094), and CD3e (553061).

Cerulein-induced Pancreatitis—10 *Adamts12*$^{+/+}$ and 9 *Adamts12*$^{-/-}$ animals were injected intraperitoneally hourly with 50 μg of cerulein (Sigma)/kg of body weight for 10 h. Untreated controls were treated with saline solution solely. One hour after the last injection, animals were anesthetized, and blood was obtained by intracardiac puncture and pancreas isolated. Serum levels of amylase and lipase were determined enzymatically in a Cobas 6000 analyzer (Roche Diagnostics).

Analysis of Cytokine Levels in Colonic Lavages—After colon extraction, 1 ml of PBS was passed three times through the large intestine. Protein concentration was quantified using the BCA Protein Assay kit (Pierce), and 30 μg of total protein from each sample was used in subsequent experiments. To select cytokines showing differences between both genotypes, we performed a preliminary analysis using the Multi-Analyte ELISArray (Tebu-bio), and those exhibiting differences were further analyzed in eight animals per genotype and time point using ELISA kits for detection of IL-1α, IL-6, and G-CSF (Tebu-bio) following the manufacturer's instructions.

Histological Analyses and Myeloperoxidase (MPO) Immunohistochemistry—Tissue samples were fixed with 4% formaldehyde for 24 h, washed with 70% ethanol, and embedded in paraffin. Sections were stained with hematoxylin and eosin and analyzed by an expert pathologist. For interacinar septa quantification, we performed six measurements per animal slide with ImageJ software. The number of polymorphonuclear cells was determined by MPO immunohistochemical detection. The reaction was carried out with an anti-MPO antibody (Thermo Fisher Scientific) in the Discovery XT System (Ventana). First, unmasking was performed by heating at pH 8.4 with CC1 buffer. Then, slides were blocked with the casein-based antibody block and incubated with the antibody at 37 °C, for 1 h and at 1:50 dilution in antibody diluent. The secondary antibody used was OmniMap anti-rabbit horseradish peroxidase, and detection was carried out with ChromoMap DAB. Contrast staining was performed with hematoxylin and bluing reagent (all reagents from Ventana). After staining, the number of MPO-positive cells in equivalent areas of ulceration was determined in slides from *Adamts12*-proficient and -deficient mice (6 fields/slide, $n = 4$/group).

RNA Expression Arrays—Whole RNA from colon was isolated using TRIzol (Invitrogen) and purified with the RNeasy Mini Kit (Qiagen). Concentration and quality of samples were

determined using an Agilent 2100 Bioanalyzer, and those with the best quality were selected for hybridization with GeneChip Mouse Gene 1.0 ST Arrays (Affymetrix), following the manufacturer's instructions. Quality control of microarray data was performed using Affymetrix Expression Console. Data are expressed as base 2 exponentials. Array data were deposited at the Gene Expression Omnibus with the accession number GSE40529. Bioinformatic analysis was performed using the Babelomics platform.

Proteomic Studies and MALDI-ToF Analysis—Colons from *Adamts12*$^{-/-}$ and *Adamts12*$^{+/+}$mice were homogenized in TUCT (7 M urea, 2 M thiourea, 4% CHAPS, and 30 mM Tris-HCl, pH 8.5). 50 μg of each sample were labeled with 400 pmol of a specific fluorophore (GE Healthcare): CyDye 3 (WT sample), CyDye 5 (KO sample), and CyDye 2 (pool of WT and KO samples 1:1). Labeled samples were combined, and UCDA (8 M urea, 4% CHAPS, 130 mM DTT and 2% isoelectrofocusing (IEF) buffer) was added in a 1:1 ratio. Then, UCda (8 M urea, 4% CHAPS, 13 mM DTT, and 1% IEF buffer) was added up to 450 μl final volume. Samples were loaded in a strip holder, and a 24-cm immobilized pH gradient (IPG) strip, pH gradient 3–11 nonlinear (GE Healthcare), was placed over it. IEF was performed for 26 h at a gradient voltage on an IPGphor Unit (GE Healthcare). Then, the strip was equilibrated in SES-DTT (6 M urea, 30% glycerol, 2% SDS, 75 mM Tris-HCl, pH 6.8, 0.5% DTT, and bromphenol blue), and in SES-IA (6 M urea, 30% glycerol, 2% SDS, 75 mM Tris-HCl, pH 6.8, 4.5% iodoacetamide, and bromphenol blue) and mounted on top of a 13% SDS-PAGE in a Hoefer S600 device (Ettan DALT Six; GE Healthcare). After SDS-PAGE, CyDye-labeled proteins were visualized directly by scanning using a Typhoon^{TM} 9400 imager (GE Healthcare). The excitation laser wavelengths were 488 nm for Cy2, 532 for Cy3, and 633 for Cy5. The emission filters employed were of 520 nm band pass 40, 580 nm band pass 30, and 670 nm band pass 30, respectively. The gel was scanned, analyzed with Progenesis SameSpots software (NonLinear Dynamics), and stained with SYPRO Ruby (Invitrogen). Differential spots were excised, washed with 25 mM ammonium bicarbonate/acetonitrile (70:30), dried, and incubated with 12 ng/μl trypsin (Promega) in 25 mM ammonium bicarbonate for 1 h at 60 °C. Peptides were purified with ZipTip C18 (Millipore), eluted with 1 μl of α-cyano-4-hydroxycinnamic acid (Waters), and analyzed by mass spectrometry on a time-of-flight mass spectrometer (Voyager-DE STR; Applied Biosystems). Data from 200 laser shots were collected to produce a mass spectrum that was analyzed with Data explorer version 4.0.0.0 (Applied Biosystems).

Western Blotting—Proteins were separated by electrophoresis and transferred to polyvinylidene difluoride membranes (Millipore). Blots were blocked with 5% nonfat dry milk in TBS-T buffer (20 mM Tris-HCl, pH 7.4, 150 mM NaCl, and 0.05% Tween 20) for 1 h at room temperature and incubated overnight at 4 °C with 3% BSA in TBS-T with either 2 μg/ml anti-galectin-1 or 0.2 μg/ml anti-S100A8 or anti-S100A9 (R&D Systems); 5% BSA with 0.2 μg/ml anti-S100A6 (R&D Systems); and in 3% nonfat dry milk in TBS-T buffer with 0.2 μg/ml anti-transgelin (ProteinTech), 0.2 μg/ml anti-hemopexin or 0.2 μg/ml anti-calgranulin A/B (Santa Cruz Biotechnology). Blots were then incubated with 10 ng/ml rabbit anti-goat horseradish peroxidase (Jackson ImmunoResearch), donkey anti-rabbit horseradish peroxidase (GE Healthcare), and goat anti-mouse horseradish peroxidase (Jackson ImmunoResearch), respectively. Finally, blots were washed with TBS-T and developed with Immobilon Western chemiluminescent HRP substrate (Millipore). Chemiluminescent images were taken in a Fujifilm LAS3000 mini.

Neutrophil Isolation and Culture—Neutrophils from *Adamts12*$^{-/-}$ and *Adamts12*$^{+/+}$ mice were isolated from peritoneal lavage as described previously (15). Cells were then washed and levels of apoptotic neutrophils determined by flow cytometry in a Cytomics FC500 (Beckman-Coulter), as annexin V- and Ly6G-positive cells using the anti-Ly6G antibody and the annexin V-FITC/propidium iodide (PI) kit (APOAF-50TST 047K4115; Sigma). For co-culture with ADAMTS-12-overexpressing cells, human neutrophils were isolated from peripheral blood of healthy donors under informed consent. Briefly, 4 ml of blood was mixed with 4 ml of a sterile solution of 0.9% NaCl. Diluted blood was then added to 4 ml of Lymphoprep^{TM} and centrifuged for 20 min at 800 relative centrifugal force. After separation, supernatant was removed, and the pellet containing granulocytes and erythrocytes was suspended in 12 ml of erythrocyte lysis buffer (150 mM NH_4Cl, 10 mM $KHCO_3$, 0.1 mM EDTA). After 10 min, this suspension was centrifuged for 5 min at 400 relative centrifugal force; supernatant was removed, and the remaining pellet was washed with 800 μl of erythrocyte lysis buffer. The final pellet containing purified granulocytes (mainly neutrophils) was resuspended in RPMI 1640 medium and counted. 2×10^5 cells were co-cultured in 6-well plates with control EBNA cells or EBNA cells overexpressing ADAMTS-12 (EBNA-TS12) (7). After 15 h, neutrophils were collected, washed, and analyzed through flow cytometry to determine apoptosis levels using the annexin V-FITC/PI kit.

RT-PCR Analysis—Total RNA from tissue samples and cells was isolated using TRIzol, and reverse transcription reactions were carried out with 300 ng of RNA, using the Thermoscript RT-PCR system (Invitrogen) with random hexamers. For analysis of human *ADAMTS12* expression, 9 μl of a 1:5 dilution of cDNA was employed in quantitative PCR using the TaqMan probe HS00917112_m1 and TaqMan Master Mix in an Abi-Prism 7900HT (Applied Biosystems) and following the manufacturer's instructions. In the case of murine *Adamts12*, 2 μl of cDNA was used as template for further amplification employing Platinum *Taq* polymerase (Invitrogen) and the specific primers 5′-CGTGGAGTCGTACATCCTCAC-3′ (forward) and 5′-CCCACGGGCTCACAGTCATTT-3′ (reverse), which amplify a 441-bp fragment. PCR amplifications were performed under the following conditions: one cycle at 94 °C for 2 min, and 35 cycles at 94 °C for 30 s, 58 °C for 30 s, and 72 °C for 30 s. β-Actin was amplified as an internal control.

Statistical Analysis—All statistical analysis were carried out with the GraphPad Prism 5.0 software. Data are presented as means ± S.E. The occurrence of significant differences between groups was determined with the Student's *t* test (for Gaussian distributions) or the Mann-Whitney test (nonparametric). Survival curves were compared using the Gehan-Breslow-Wilcoxon test. *p* values under 0.05 were considered significant (*, $p < 0.05$; **, $p < 0.01$; ***, $p < 0.001$).

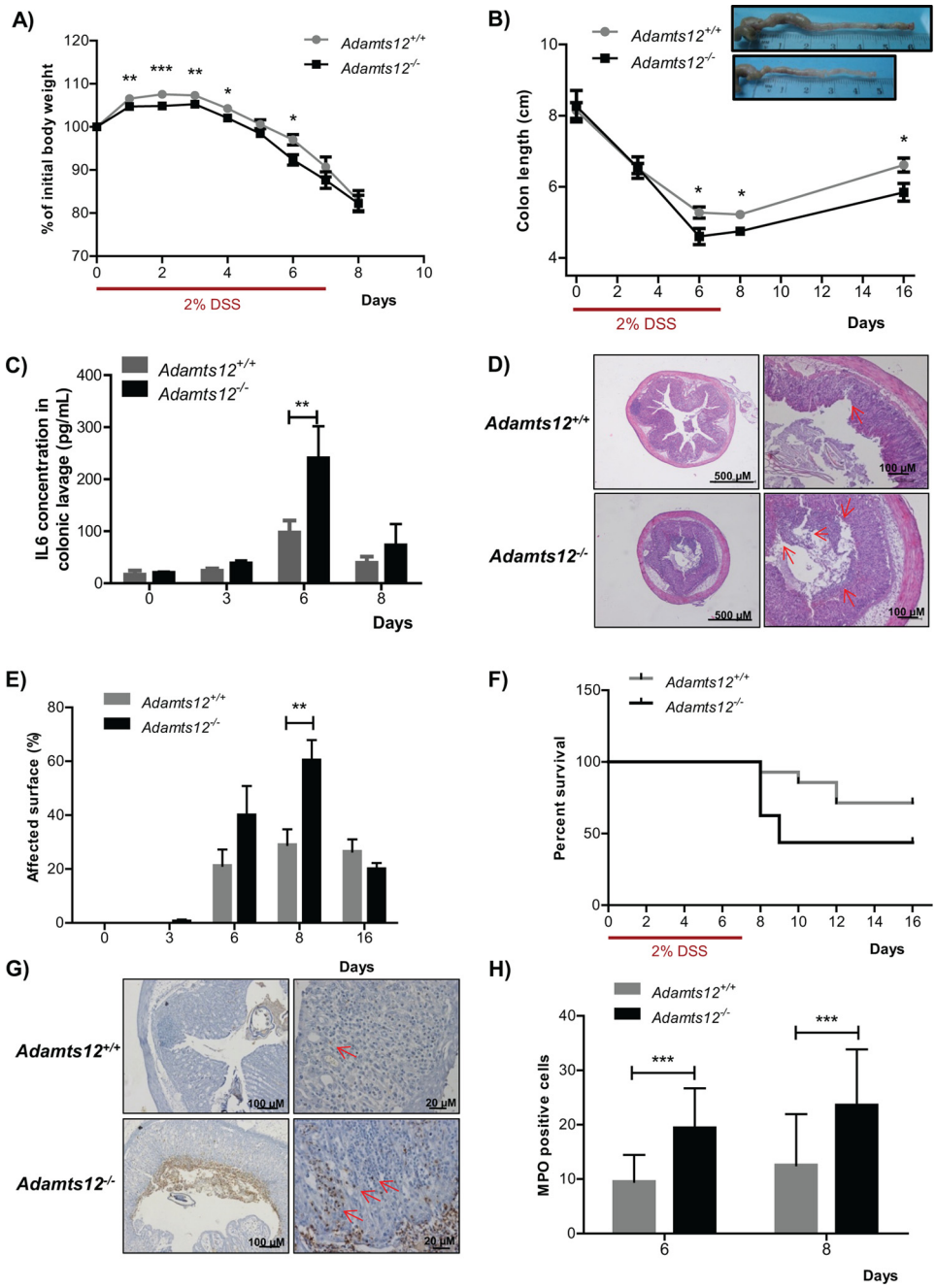

FIGURE 1. **Increased susceptibility of *Adamts12*-deficient mice to colitis.** *A*, increased body weight reduction of *Adamts12*$^{-/-}$ mice during colitis. Weights are expressed as means of individual data relative to initial body weight of each animal. *B*, colon length at time of sacrifice prior or during 2% DSS treatment. *C*, levels of IL-6 in colonic lavage as determined by ELISA. *D*, microscopic images of colonic mucosa stained with hematoxylin and eosin at day 8 after DSS treatment in mice from both genotypes. Ulcerated surface, more abundant in KO tissue, is indicated with *red arrows*. *E*, percentage of colonic surface affected by ulcers at days 0, 3, 6, 8, and 16. *F*, Kaplan-Meier plot of *Adamts12*$^{+/+}$ and *Adamts12*$^{-/-}$ during DSS-induced colitis. Comparison of survival curves for both genotypes using the Gehan-Breslow-Wilcoxon test revealed that mortality was significantly higher in KO animals (p value = 0.0454). *G*, representative images of MPO staining in DSS-treated colons at day 8. *Red arrows* indicate some of the MPO-positive cells. *H*, quantification of MPO-positive brown cells per field in affected mucosa at days 6 and 8 of treatment. *, $p < 0.05$; **, $p < 0.01$; ***, $p < 0.001$. Results are expressed as means ± S.E. (*error bars*).

RESULTS

Adamts12 Deficiency Results in Increased Inflammation and Higher Susceptibility to DSS-induced Colitis—Whereas no significant differences were observed in clinical features (diarrhea and rectal bleeding), we detected increased weight loss in *Adamts12*$^{-/-}$ mice during DSS treatment (Fig. 1*A*). Likewise, significantly reduced colon length, a symptom of inflammation, was also observed in knock-out (KO) mice compared with wild-type (WT) at days 6 (mean WT = 5.28 ± 0.16; KO = 4.60 ± 0.22) and 8 (mean WT = 5.22 ± 0.11; KO = 4.75 ± 0.12) (Fig. 1*B*). The degree of inflammation was also evaluated in terms of cytokine abundance in colonic lavage. We found enhanced levels of IL-1α, IL-6, and G-CSF in *Adamts12*-deficient mice, with these differences being significant at day 6 for IL-6 (Fig. 1*C* and supplemental Fig. 1). Histological examination of colon revealed that the extent of surface affected by ulcers was higher

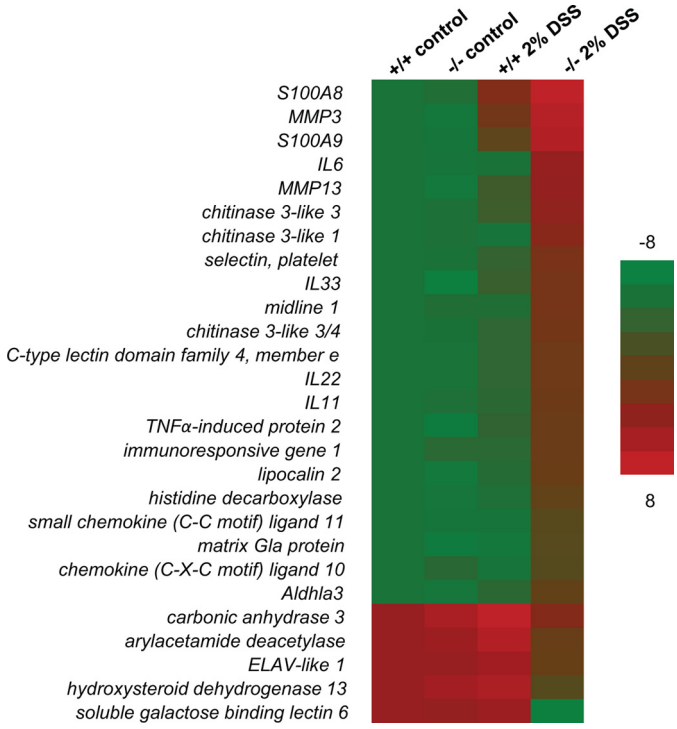

FIGURE 2. **Microarray analysis in colon from *Adamts12*$^{+/+}$ and *Adamts12*$^{-/-}$ mice.** Heat map represents the relative expression levels of selected genes as determined by hybridization with GeneChip Mouse Gene 1.0 ST Arrays.

in *Adamts12*$^{-/-}$ animals, especially at day 8 (mean 52.5% in mutant mice *versus* 30.6% in controls) (Fig. 1, *D* and *E*). To study putative differences regarding mortality, we treated another group of animals and observed that mortality was increased in *Adamts12*-deficient mice compared with control littermates (Fig. 1*F*). Once these mice had recovered their initial body weight (at day 16), they were sacrificed, and although no apparent differences were observed at the histological level, colons from *Adamts12*$^{-/-}$ were still significantly shortened (Fig. 1*B*).

Increased Inflammation in Adamts12$^{-/-}$ *Mice Colon Is Associated with Neutrophil Accumulation*—Examination of areas of ulceration with an anti-MPO antibody revealed a marked increase in neutrophil infiltration in *Adamts12*-deficient tissue (Fig. 1*G*). Quantitative analysis confirmed a significant increase in the number of positive cells per field ($p < 0.0001$, *Adamts12*$^{-/-}$ mean = 19.38 ± 1.49 at day 6 and 23.58 ± 1.48 at day 8; *Adamts12*$^{+/+}$ mean = 9.50 ± 1.01 at day 6 and 12.56 ± 1.36 at day 8) (Fig. 1*H*). The sustained presence of neutrophils in colon would generate a pro-inflammatory environment that could contribute to explain the exacerbated affectation observed in DSS-treated *Adamts12*$^{-/-}$.

Several Inflammation Markers Are Elevated at the Transcriptional and Proteomic Levels in the Absence of Adamts12—mRNA profiles from affected colons at day 8 of *Adamts12*$^{-/-}$ mice revealed augmented expression of several inflammation markers. Of the >28,000 genes analyzed, we selected 21 whose expression was similar between genotypes when untreated (differing in <2-fold) but overexpressed ~6 or more times in mutant animals under DSS treatment (Fig. 2). Bioinformatic analysis to identify enrichment of functionally related genes revealed an enrichment of genes involved in the cytokine and cytokine-receptor interaction ($p = 4.2 \times 10^{-6}$) and of genes expressed during hematopoiesis, specifically in the neutrophil lineage ($p = 6.63 \times 10^{-7}$). This group of genes includes those encoding several interleukins, the calgranulins S100A8 and S100A9, and the chemokines Ccl11 or Cxcl10. Additionally, *Hdc* and *Aldhla3* genes necessary for histamine synthesis and metabolism, as well as MMP genes that have also been related to inflammation (16, 17), such as *Mmp3* and *Mmp13*, were increased in KO mice. Notably, IL-6, one of the overexpressed cytokines in mutant mice and also found accumulated at the colonic lavage of these animals (Fig. 1*C*), has been traditionally considered as a marker of inflammatory bowel disease severity (18–21). Finally, it is remarkable that few genes were found to be down-regulated in *Adamts12*-deficient mice and were not ascribable to specific functions. This is the case of *LgalS6*, a galectin present in murine gastrointestinal tract and of arylacetamide deacetylase and hydroxysteroid dehydrogenase 13, which encode enzymes participant in metabolic processes.

We then explored putative differences at the protein level. For this purpose, we performed a two-dimensional DiGE combined with MALDI-ToF analysis of colon samples from *Adamts12*$^{-/-}$ and *Adamts12*$^{+/+}$ animals treated with DSS at day 8. We identified several proteins, including galectin-1, hemopexin, transgelin, S100A6, S100A8, and S100A9, accumulated in KO tissues (Fig. 3*A*). These results were validated through two-dimensional Western blotting (Fig. 3*B*). S100A8 and S100A9 were also found increased at the mRNA level, reinforcing the above results and ruling out a protein accumulation caused by a putative absence of proteolytic processing by Adamts-12. None of the other mentioned proteins were found transcriptionally overexpressed. Further one-dimensional Western blotting confirmed that S100A8, S100A9, and hemopexin were uniformly accumulated in all KO tissues at days 6 and 8 of treatment (no significant differences were evident at day 3) (Fig. 3*C* and densitometry analysis in supplemental Fig. 2, *A* and *B*). In the case of hemopexin, two-dimensional Western blots showed that the isoforms accumulated in *Adamts12*$^{-/-}$ colons were barely or not detected in samples from *Adamts12*$^{+/+}$ animals (Fig. 3*B*). This finding, together with the fact that no expression differences were found for hemopexin at the transcriptional level, suggests that Adamts-12 could be involved in the post-translational processing of hemopexin. Finally, calprotectin, a heterodimeric complex formed by combination of S100A8 and S100A9, was also accumulated in KO tissues at day 8 (Fig. 3*C*, *right panel*).

Adamts12$^{-/-}$ *Mice Show Delayed Recovery after LPS-induced Sepsis*—Next, we analyzed the Adamts-12 role in a model of global acute inflammation, by comparing the host response to LPS-induced sepsis. Although no significant differences were observed regarding mortality or weight loss, we noticed significant differences affecting different blood parameters. Thus, we detected an increased hematocrit at day 3 and a higher number of leukocytes at day 8 in *Adamts12*$^{-/-}$ mice (Fig. 4, *A* and *B*). The enhanced hematocrit is likely due to a more severe dehydration affecting KO mice. Likewise, one of the major features achieved during sepsis is the increase of leukocytes in

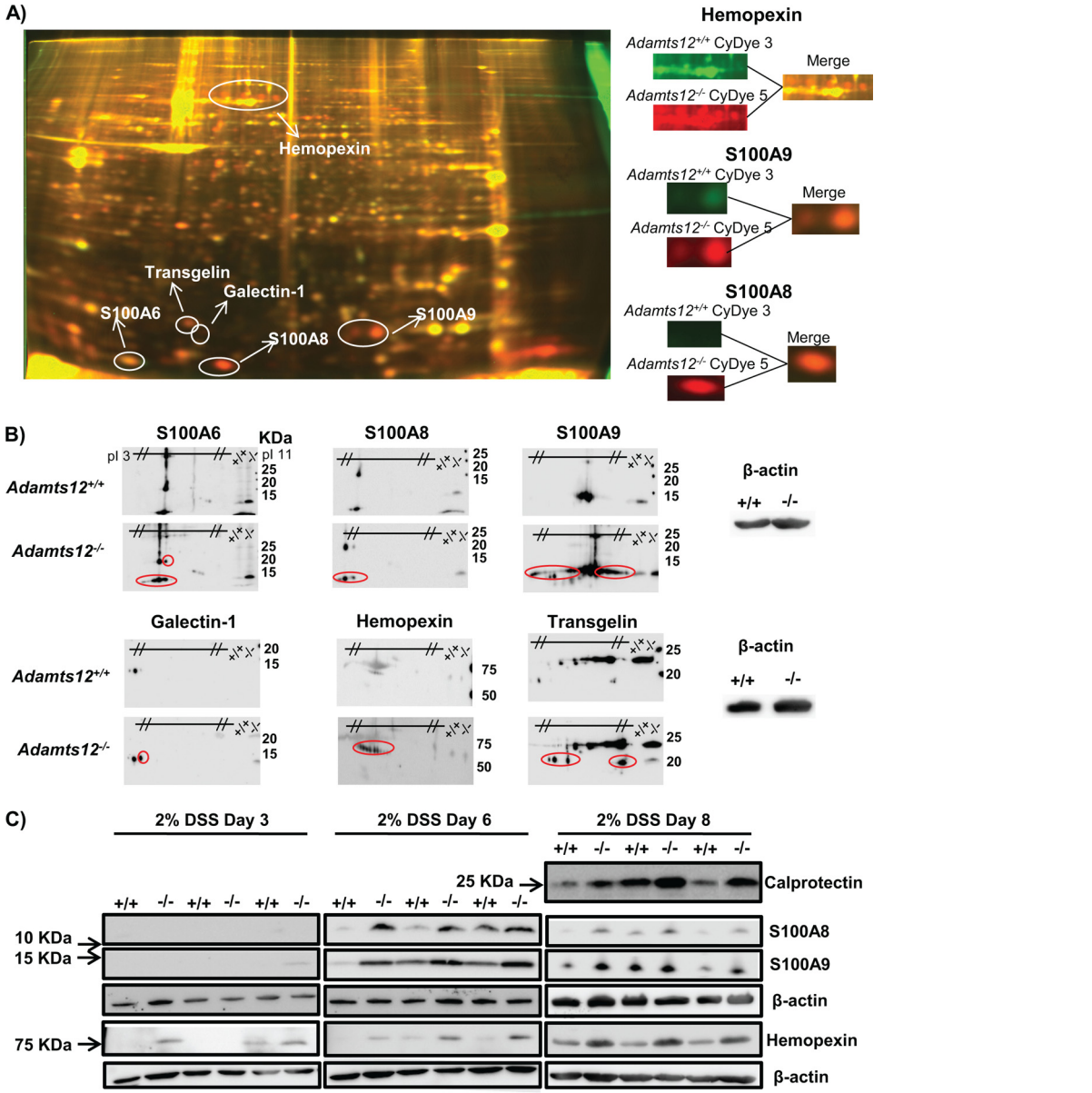

FIGURE 3. **Identification of differential proteins in colon from DSS-treated *Adamts12*$^{+/+}$ and *Adamts12*$^{-/-}$ mice.** *A*, representative DiGE image with tissue extracts from *Adamts12*$^{+/+}$ (CyDye 3, *green*) and *Adamts12*$^{-/-}$ (CyDye 5, *red*) mice. Some of the differential proteins are indicated. *B*, differentially produced proteins identified by MALDI-ToF confirmed by two-dimensional Western blotting. In each blot, uni-dimensional experiments of both *Adamts12*$^{-/-}$ and *Adamts12*$^{+/+}$ tissues are identifiable on the *right*. β-Actin was used as a loading control. *C*, Western blots detecting protein levels of those candidates identified in DiGE analysis in three representative animals per genotype and time point. S100A8, S100A9, calprotectin, and hemopexin were found to be accumulated in the absence of Adamts-12 at days 6 and 8 in two different sets of three *Adamts12*$^{-/-}$ mice compared with three *Adamts12*$^{+/+}$ animals. β-Actin was used as a loading control.

blood. In this sense, at day 8 after LPS injection, the number of white blood cells was significantly increased in *Adamts12*$^{-/-}$ mice compared with controls (Fig. 4*B*). We observed that the increment in leukocyte number at day 8 is presumably due to an increase in the number of neutrophil granulocytes (Fig. 4*C*). At day 3 after treatment, we detected changes in the percentage of each cell type: monocytes and neutrophils were more abundant in *Adamts12*-deficient mice, whereas lymphocyte number was reduced compared with WT animals (Fig. 4*C*).

We next investigated possible differences affecting the altered molecular targets identified in colitis. To this end, we performed Western blot analysis for hemopexin, S100A8 and S100A9 in protein extracts from spleen and liver of LPS-treated mice at day 8. As shown in Fig. 4*D* and supplemental Fig. 2, *C* and *D*, S100A8 and S100A9 were shown to be differential markers for *Adamts12*$^{-/-}$ also during sepsis.

Higher Affectation of Adamts12$^{-/-}$ *Mice Pancreas after Cerulein Treatment—Adamts12*$^{-/-}$ and *Adamts12*$^{+/+}$ mice were challenged with cerulein to induce pancreatitis. Mean levels of pancreatic enzymes (lipase and amylase) were higher in mutant mice compared with WT animals, although no significant differences derived from statistical analysis (levels of serum amylase were 26.45 ± 2.18 in *Adamts12*$^{+/+}$ and 29.22 ± 2.18 units/liter in *Adamts12*$^{-/-}$ mice; lipase levels were 789.0 ± 83.2 and 941.1 ± 84.5 units/liter, respectively). However, we found significantly increased edema among pancreatic

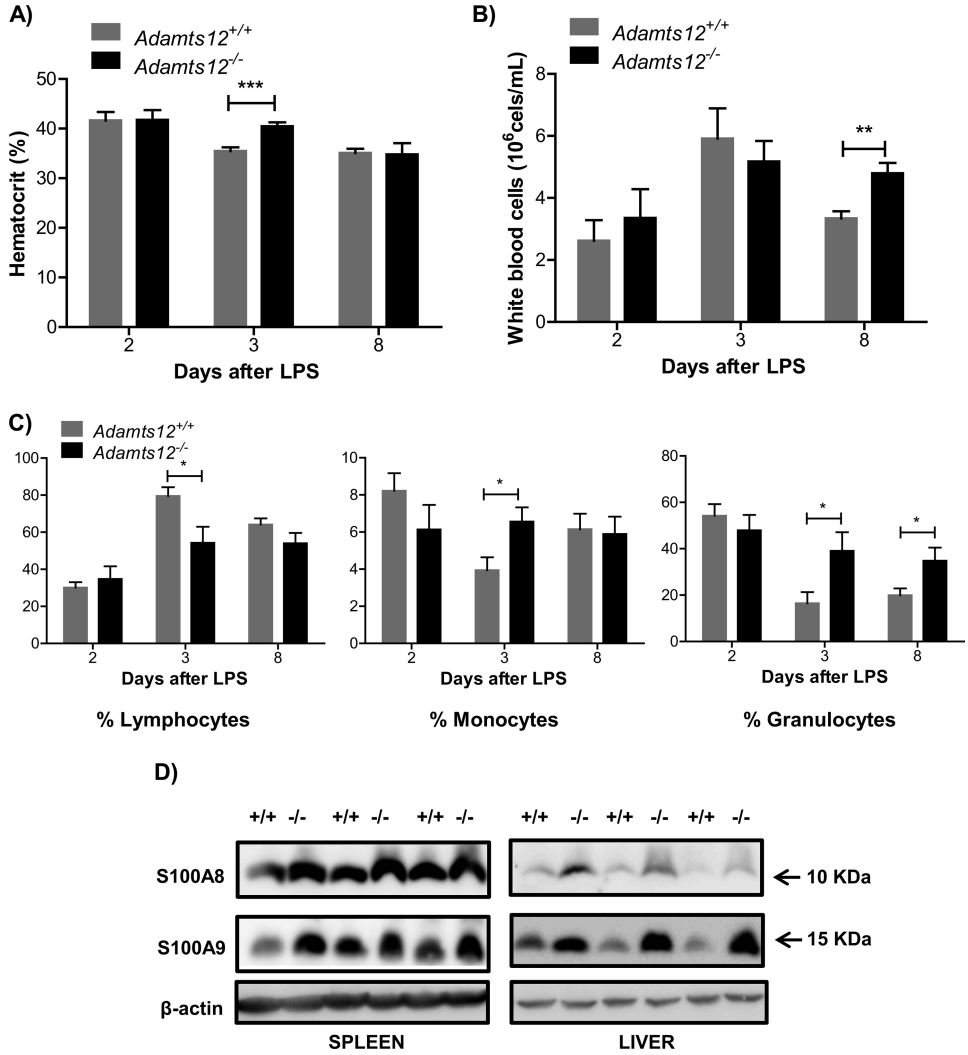

FIGURE 4. **Increased susceptibility to LPS-induced sepsis in *Adamts12*$^{-/-}$ mice.** *A*, variation in hematocrit during treatment. Mice lacking *Adamts12* show an increased hematocrit at day 3 after LPS injection, likely as an effect of more severe dehydration, compared with wild-type animals. *B*, levels of leukocytes in peripheral blood after LPS injection. At day 8 after treatment, *Adamts12*$^{-/-}$ mice show an enhanced number of leukocytes. *C*, composition of leukocyte populations in peripheral blood after LPS treatment. At day 3, an evident deviation in leukocyte populations was observed in *Adamts12*$^{-/-}$ mice, which exhibited reduced lymphocytes and increased monocytes and granulocytes compared with control animals. At day 8, the number of neutrophils was still increased in mice lacking the metalloprotease. *D*, Western blot against S100A8 and S100A9 in spleens and livers from LPS-treated mice. S100A8 and S100A9 are elevated in tissues of *Adamts12*$^{-/-}$ mice 8 days after induction of sepsis. *, $p < 0.05$; **, $p < 0.01$; ***, $p < 0.001$.

acini of specimens from *Adamts12*$^{-/-}$ mice (Fig. 5*A*). The mean interacinar distance in treated mice was 5.03 ± 0.23 μm in KO animals and 4.06 ± 0.21 μm in WT mice (Fig. 5*A*). Finally, we examined levels of S100A8, S100A9, and hemopexin in pancreas of pancreatitis-induced mice. We found an accumulation of hemopexin in *Adamts12*$^{-/-}$ tissue equivalent to that defined for colitis (Fig. 5*B* and supplemental Fig. 2*E*), although no evident differences were detected for S100A8 and S100A9.

Adamts-12 Induces Neutrophil Apoptosis—To better understand the mechanism underlying the observed effects in *Adamts12*$^{-/-}$ mice, we explored the putative link between neutrophil accumulation and the absence of this protease. In this regard, it is well known that once neutrophil activities during acute response have been completed, these cells die by cell programmed death and undergo macrophage clearance (22). Based on these considerations, we asked whether Adamts-12 could be necessary for appropriate neutrophil apoptosis. We isolated peritoneal neutrophils from *Adamts12*$^{-/-}$ and *Adamts12*$^{+/+}$ animals and analyzed their levels of apoptosis, finding a marked reduction in neutrophil apoptosis in the absence of Adamts-12: 16.79% ± 1.20 of neutrophils from WT animals were annexin V-positive *versus* 10.49% ± 1.01 from mutant mice (Fig. 6*A*).

We then asked whether this effect on apoptosis could also be detected *in vitro*. To this end, we isolated nonactivated neutrophils from blood of healthy human donors and co-cultured them for 15 h with control EBNA cells or EBNA cells overexpressing ADAMTS-12. We found that in the presence of ADAMTS-12, the percentage of apoptotic cells raised from 56.7% to 68.4% (Fig. 6*B*). From previous works (12, 13), we know that *ADAMTS12* is expressed by human myofibroblasts, which are one of the predominant cells in stroma in proinflammatory environments such as wound healing and cancer. In the models

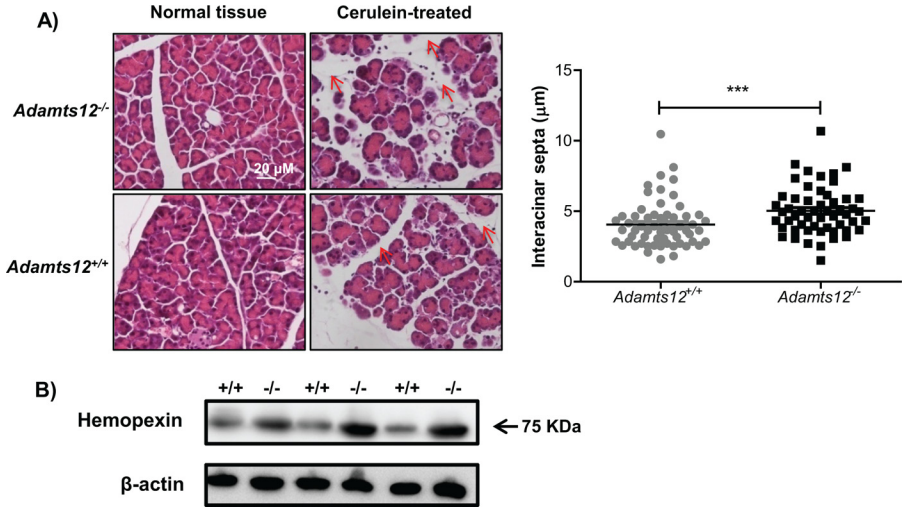

FIGURE 5. **Increased affection of *Adamts12*$^{-/-}$ mice after cerulein-induced pancreatitis.** *A*, *Adamts12*-deficient tissues are more affected by edema during pancreatitis. Microscopic images show affected pancreas stained with hematoxylin and eosin. Edema, one of the main indicators of pancreatitis, was increased in the interacinar spaces (indicated with *red arrows*) of *Adamts12*$^{-/-}$ mice after treatment with cerulein. *B*, increased levels of hemopexin in pancreatitis of mice deficient in *Adamts12*. ***, $p < 0.001$.

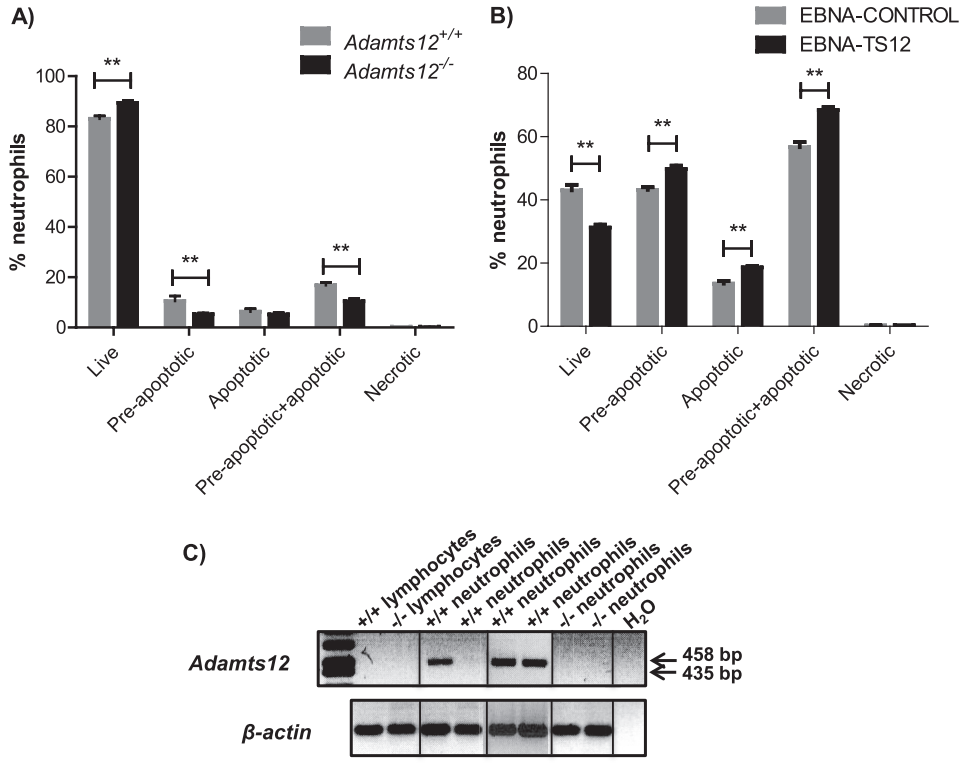

FIGURE 6. **ADAMTS-12 is expressed in neutrophils and induces their apoptosis.** *A*, apoptosis levels of peritoneal neutrophils from *Adamts12*$^{-/-}$ ($n = 7$) and *Adamts12*$^{+/+}$ ($n = 6$) mice after casein induction. *B*, percentage of live and apoptotic human neutrophils after co-culture with EBNA-TS12 or EBNA-control. Live cells are annexin V- and PI-negative; pre-apoptotic cells are annexin V-positive, PI-negative; apoptotic cells are annexin V- and PI-positive; and necrotic cells are annexin V-negative and PI-positive. *C*, RT-PCR showing murine *Adamts12* expression in cDNA from WT and KO lymphocytes and neutrophils. **, $p < 0.01$.

studied herein, ADAMTS-12 could be controlling neutrophil apoptosis through cell components of stroma, like activated fibroblasts. Nevertheless, we also asked whether neutrophils themselves could be expressing this metalloprotease. For this purpose, we performed RT-PCR and quantitative RT-PCR to analyze *ADAMTS12* expression in neutrophils from murine and human origin, respectively. Whereas *ADAMTS12* expression in lymphocytes was minimal, we detected significant expression in human (up to 7000-fold overexpression compared with lymphocytes) and murine neutrophils (Fig. 6*C* and data not shown).

DISCUSSION

The current view of proteases as modulators of precise proteolytic processing events is far away from the traditional one in which they were conceived as mere degradative enzymes in charge of protein catabolism (23, 24). Nowadays, >560 human

proteases have been identified (25). These proteases establish intimate interactions with very specific substrates and are strictly regulated over time and space through control of their expression, activity, and location. As a result, most proteases perform very specific proteolytic cleavages on a number of different substrates and influence multiple biological processes (1). Hence, predicting the phenotype of animal models deficient in a certain protease is very difficult and often offers unexpected findings. To date, several mouse models lacking ADAMTSs have been generated with a heterogeneous spectrum of phenotypes including those found in *Adamts4*- and *Adamts5*-deficient mice, which are protected from osteoarthritis (26), and in *Adamts13*-deficient mice, which show increased inflammation due to enhanced extravasation of neutrophils (27).

In the present work, we have found that loss-of-function of Adamts-12 enhances mouse susceptibility to inflammatory processes. This phenotype was not limited to a certain tissue as it was a common phenomenon affecting several organs. Thus, mice lacking *Adamts12* exhibited an increased damage subsequent to inflammation in colon and pancreas and during endotoxic shock. Particularly, *Adamts12*$^{-/-}$ mice subjected to induction of experimental colitis showed a more pronounced loss of weight, colon shortening, and epithelial ulceration. Similar results were observed during pancreatitis, as histopathological analysis of pancreas revealed a more pronounced edema in tissues from mutant mice. Additionally, induction of systemic sepsis highlighted the higher inflammatory response taking place in *Adamts12*-deficient mice. Further gene expression and proteomic studies confirmed and extended these differences, as most differential RNAs and proteins identified in these mutant mice are indicators of increased inflammation. These were the cases with the pro-inflammatory cytokines IL-6, IL-11, or CCL-11, and the calcium-binding proteins S100A8 and S100A9, important amplifiers and markers of acute and chronic inflammation (28), which were increased at both RNA and protein level in *Adamts12*-deficient mice. The latter two proteins form the heterodimer calprotectin, currently used as a diagnostic indicator for inflammatory bowel diseases when present in feces, and which was also found accumulated in colons from *Adamts12*$^{-/-}$ mice exposed to DSS. Taken collectively, all of these observations indicate that Adamts-12 is necessary for a normal inflammatory response in mice.

We also found that the more severe inflammatory symptoms observed in *Adamts12*-deficient mice were accompanied by neutrophilia in the affected tissues, which provided us a first clue to initiate the search for the mechanism underlying the phenotypic and molecular differences present in these mutant mice. In normal conditions, and immediately after a harmful stimulus, neutrophils migrate toward the affected tissue and contribute to the development of an immune response. Thus, these cells produce pro-inflammatory cytokines that attract other inflammatory cells and amplify the response as well as release toxic substances aimed at eliminating pathogens. Nevertheless, when this delicate balance is altered and excessive neutrophils are present, they can promote chronic inflammation and directly cause damage to the host tissue (29). Normally, after neutrophils exert their function in the acute phase response, they suffer massive apoptosis and are phagocytosed by macrophages (22). On this basis, we hypothesized that a defect in apoptosis in the absence of Adamts-12 could be responsible for the increased number of neutrophils. To test this possibility, we analyzed changes in apoptotic death in neutrophils from human and murine origin, with the finding that the presence of this metalloprotease triggered an increment in their apoptosis. In this regard, previous works have described the ability of proteins containing thrombospondin type-1 repeats to interact with surface proteins such as CD36 and CD47 (30, 31), that can modulate neutrophil death and clearance (32, 33). Hence, it is conceivable a model in which ADAMTS-12 could participate in similar protein interactions through its thrombospondin domains. Alternatively, we have found that some hemopexin isoforms were accumulated in *Adamts12*-deficient mice (Fig. 3, *A* and *B*), which may suggest an implication of this metalloprotease on hemopexin processing. If this were the case, the absence of *Adamts12* could lead to an altered function of hemopexin, which is mainly involved in sequestering the extracellular free heme and in its recovery in liver (34). Free heme is released during several types of cell damage, causing oxidative effects and promoting inflammation. Indeed, it has been proven that heme is able to delay spontaneous apoptosis of human neutrophils (35). Additionally, two of the cytokines found increased in *Adamts12* KO mice, IL-6 and G-CSF, have also been related to neutrophil apoptosis and survival. G-CSF has been described as a potent promoter of neutrophil durability (36) and may be acting in this context as one of the mediators for neutrophil death inhibition. Conversely, IL-6 allows the successful transition from innate to adaptive response by limiting neutrophil recruitment (37), and its increased levels in *Adamts12*-deficient mice could be part of a homeostatic response to the excessive neutrophilia, otherwise inefficient due to the impaired apoptosis. Finally, ADAMTS-12 might be involved in other processes apart from neutrophil apoptosis, such as neovascularization or matrix remodeling, which contribute to normal healing of ulcers in colitis. All of these results are preliminary but relevant evidences of the molecular mechanisms by which ADAMTS-12 exerts its role in inflammation. Nevertheless, all of the proposed hypothesis are conjectural and may be clarified in future experiments.

In summary, in this work we provide evidence on how *Adamts12* deficiency is responsible for increased inflammation in mice and reduced apoptosis of neutrophils. Furthermore, we know from previous studies that Adamts-12 is also implicated in angiogenesis, apoptosis of tumor cells and modification of the extracellular matrix (7, 12, 14). Therefore, albeit Adamts-12 is not essential for life, probably due to functional compensation by other ADAMTSs, the contribution of this enzyme to a variety of inflammatory processes highlights its relevance in the context of the large and growing complexity of proteolytic systems operating in life and disease.

Acknowledgments—We thank A. R. Folgueras, J. M. P. Freije, and A. Fueyo for helpful comments; F. V. Alvarez for biochemical determinations; A. Salas for FACS analysis; A. Fernández, S. Fernández, and M. S. Pitiot for histopathological studies; and S. Alvarez for excellent technical assistance.

REFERENCES

1. López-Otin, C., and Bond, J. S. (2008) Proteases: multifunctional enzymes in life and disease. *J. Biol. Chem.* **283,** 30433–30437
2. Apte, S. S. (2009) A disintegrin-like and metalloprotease (reprolysin-type) with thrombospondin type 1 motif (ADAMTS) superfamily: functions and mechanisms. *J. Biol. Chem.* **284,** 31493–31497
3. Cal, S., Obaya, A. J., Llamazares, M., Garabaya, C., Quesada, V., and López-Otin, C. (2002) Cloning, expression analysis, and structural characterization of seven novel human ADAMTSs, a family of metalloproteinases with disintegrin and thrombospondin-1 domains. *Gene* **283,** 49–62
4. Lin, E. A., and Liu, C. J. (2010) The role of ADAMTSs in arthritis. *Protein Cell* **1,** 33–47
5. Renz, H., von Mutius, E., Brandtzaeg, P., Cookson, W. O., Autenrieth, I. B., and Haller, D. (2011) Gene-environment interactions in chronic inflammatory disease. *Nat. Immunol.* **12,** 273–277
6. Cal, S., Arguelles, J. M., Fernandez, P. L., and López-Otin, C. (2001) Identification, characterization, and intracellular processing of ADAM-TS12, a novel human disintegrin with a complex structural organization involving multiple thrombospondin-1 repeats. *J. Biol. Chem.* **276,** 17932–17940
7. Llamazares, M., Obaya, A. J., Moncada-Pazos, A., Heljasvaara, R., Espada, J., López-Otin, C., and Cal, S. (2007) The ADAMTS12 metalloproteinase exhibits anti-tumorigenic properties through modulation of the Ras-dependent ERK signalling pathway. *J. Cell Sci.* **120,** 3544–3552
8. Liu, C. J., Kong, W., Xu, K., Luan, Y., Ilalov, K., Sehgal, B., Yu, S., Howell, R. D., and Di Cesare, P. E. (2006) ADAMTS-12 associates with and degrades cartilage oligomeric matrix protein. *J. Biol. Chem.* **281,** 15800–15808
9. Nah, S. S., Lee, S., Joo, J., Kim, H. K., Sohn, D. R., Kwon, J. T., Woo, K. M., Hong, S. J., and Kim, H. J. (2012) Association of ADAMTS12 polymorphisms with rheumatoid arthritis. *Mol. Med. Report* **6,** 227–231
10. Kurz, T., Hoffjan, S., Hayes, M. G., Schneider, D., Nicolae, R., Heinzmann, A., Jerkic, S. P., Parry, R., Cox, N. J., Deichmann, K. A., and Ober, C. (2006) Fine mapping and positional candidate studies on chromosome 5p13 identify multiple asthma susceptibility loci. *J. Allergy Clin. Immunol.* **118,** 396–402
11. Bespalova, I. N., Angelo, G. W., Ritter, B. P., Hunter, J., Reyes-Rabanillo, M. L., Siever, L. J., and Silverman, J. M. (2012) Genetic variations in the *ADAMTS12* gene are associated with schizophrenia in Puerto Rican patients of Spanish descent. *Neuromolecular Med.* **14,** 53–64
12. Moncada-Pazos, A., Obaya, A. J., Fraga, M. F., Viloria, C. G., Capellá, G., Gausachs, M., Esteller, M., López-Otin, C., and Cal, S. (2009) The *ADAMTS12* metalloprotease gene is epigenetically silenced in tumor cells and transcriptionally activated in the stroma during progression of colon cancer. *J. Cell Sci.* **122,** 2906–2913
13. Wang, D., Zhu, T., Zhang, F. B., and He, C. (2011) Expression of *ADAMTS12* in colorectal cancer-associated stroma prevents cancer development and is a good prognostic indicator of colorectal cancer. *Digest. Dis. Sci.* **56,** 3281–3287
14. El Hour, M., Moncada-Pazos, A., Blacher, S., Masset, A., Cal, S., Berndt, S., Detilleux, J., Host, L., Obaya, A. J., Maillard, C., Foidart, J. M., Ectors, F., Noel, A., and Lopez-Otin, C. (2010) Higher sensitivity of *Adamts12*-deficient mice to tumor growth and angiogenesis. *Oncogene* **29,** 3025–3032
15. Luo, Y., and Dorf, M. E. (2001) Isolation of mouse neutrophils. *Curr. Protoc. Immunol.* **Chapter 3,** Unit 3.20
16. Warner, R. L., Bhagavathula, N., Nerusu, K. C., Lateef, H., Younkin, E., Johnson, K. J., and Varani, J. (2004) Matrix metalloproteinases in acute inflammation: induction of MMP-3 and MMP-9 in fibroblasts and epithelial cells following exposure to pro-inflammatory mediators *in vitro*. *Exp. Mol. Pathol.* **76,** 189–195
17. Sen, A. I., Shiomi, T., Okada, Y., and D'Armiento, J. M. (2010) Deficiency of matrix metalloproteinase-13 increases inflammation after acute lung injury. *Exp. Lung Res.* **36,** 615–624
18. Mitsuyama, K., Sasaki, E., Toyonaga, A., Ikeda, H., Tsuruta, O., Irie, A., Arima, N., Oriishi, T., Harada, K., and Fujisaki, K. (1991) Colonic mucosal interleukin-6 in inflammatory bowel disease. *Digestion* **50,** 104–111
19. Carey, R., Jurickova, I., Ballard, E., Bonkowski, E., Han, X., Xu, H., and Denson, L. A. (2008) Activation of an IL-6:STAT3-dependent transcriptome in pediatric-onset inflammatory bowel disease. *Inflamm. Bowel Dis.* **14,** 446–457
20. Li, Y., de Haar, C., Chen, M., Deuring, J., Gerrits, M. M., Smits, R., Xia, B., Kuipers, E. J., and van der Woude, C. J. (2010) Disease-related expression of the IL6/STAT3/SOCS3 signalling pathway in ulcerative colitis and ulcerative colitis-related carcinogenesis. *Gut* **59,** 227–235
21. Wang, K., Yuan, C. P., Wang, W., Yang, Z. Q., Cui, W., Mu, L. Z., Yue, Z. P., Yin, X. L., Hu, Z. M., and Liu, J. X. (2010) Expression of interleukin 6 in brain and colon of rats with TNBS-induced colitis. *World J. Gastroenterol.* **16,** 2252–2259
22. Bratton, D. L., and Henson, P. M. (2011) Neutrophil clearance: when the party is over, clean-up begins. *Trends Immunol.* **32,** 350–357
23. López-Otin, C., and Overall, C. M. (2002) Protease degradomics: a new challenge for proteomics. *Nat. Rev. Mol. Cell. Biol.* **3,** 509–519
24. López-Otin, C., and Hunter, T. (2010) The regulatory crosstalk between kinases and proteases in cancer. *Nat. Rev. Cancer* **10,** 278–292
25. Quesada, V., Ordóñez, G. R., Sánchez, L. M., Puente, X. S., and López-Otin, C. (2009) The Degradome database: mammalian proteases and diseases of proteolysis. *Nucleic Acids Res.* **37,** D239–243
26. Majumdar, M. K., Askew, R., Schelling, S., Stedman, N., Blanchet, T., Hopkins, B., Morris, E. A., and Glasson, S. S. (2007) Double-knockout of *ADAMTS-4* and *ADAMTS-5* in mice results in physiologically normal animals and prevents the progression of osteoarthritis. *Arthritis Rheum.* **56,** 3670–3674
27. Chauhan, A. K., Kisucka, J., Brill, A., Walsh, M. T., Scheiflinger, F., and Wagner, D. D. (2008) *ADAMTS13*: a new link between thrombosis and inflammation. *J. Exp. Med.* **205,** 2065–2074
28. Gebhardt, C., Németh, J., Angel, P., and Hess, J. (2006) S100A8 and S100A9 in inflammation and cancer. *Biochem. Pharmacol.* **72,** 1622–1631
29. Lonkar, P., and Dedon, P. C. (2011) Reactive species and DNA damage in chronic inflammation: reconciling chemical mechanisms and biological fates. *Int. J. Cancer* **128,** 1999–2009
30. Davis, A. K., Makar, R. S., Stowell, C. P., Kuter, D. J., and Dzik, W. H. (2009) ADAMTS13 binds to CD36: a potential mechanism for platelet and endothelial localization of ADAMTS13. *Transfusion* **49,** 206–213
31. Lamy, L., Foussat, A., Brown, E. J., Bornstein, P., Ticchioni, M., and Bernard, A. (2007) Interactions between CD47 and thrombospondin reduce inflammation. *J. Immunol.* **178,** 5930–5939
32. Mikolajczyk, T. P., Skrzeczyńska-Moncznik, J. E., Zarebski, M. A., Marewicz, E. A., Wiśniewska, A. M., Dzieba, M., Dobrucki, J. W., and Pryjma, J. R. (2009) Interaction of human peripheral blood monocytes with apoptotic polymorphonuclear cells. *Immunology* **128,** 103–113
33. Lawrence, D. W., King, S. B., Frazier, W. A., and Koenig, J. M. (2009) Decreased CD47 expression during spontaneous apoptosis targets neutrophils for phagocytosis by monocyte-derived macrophages. *Early Hum. Dev.* **85,** 659–663
34. Hvidberg, V., Maniecki, M. B., Jacobsen, C., Højrup, P., Møller, H. J., and Moestrup, S. K. (2005) Identification of the receptor scavenging hemopexin-heme complexes. *Blood* **106,** 2572–2579
35. Arruda, M. A., Rossi, A. G., de Freitas, M. S., Barja-Fidalgo, C., and Graça-Souza, A. V. (2004) Heme inhibits human neutrophil apoptosis: involvement of phosphoinositide 3-kinase, MAPK, and NF-κB. *J. Immunol.* **173,** 2023–2030
36. Maianski, N. A., Roos, D., and Kuijpers, T. W. (2004) Bid truncation, bid/bax targeting to the mitochondria, and caspase activation associated with neutrophil apoptosis are inhibited by granulocyte colony-stimulating factor. *J. Immunol.* **172,** 7024–7030
37. Fielding, C. A., McLoughlin, R. M., McLeod, L., Colmont, C. S., Najdovska, M., Grail, D., Ernst, M., Jones, S. A., Topley, N., and Jenkins, B. J. (2008) IL-6 regulates neutrophil trafficking during acute inflammation via STAT3. *J. Immunol.* **181,** 2189–2195